Normal and quasinormal modes of holographic multiquark star

Supakchai Ponglertsakul,[1,*] Piyabut Burikham,[2,†] and Sitthichai Pinkanjanarod[3,‡]

[1]*Strong Gravity Group, Department of Physics, Faculty of Science, Silpakorn University, Nakhon Pathom 73000, Thailand*

[2]*High Energy Physics Theory Group, Department of Physics, Faculty of Science, Chulalongkorn University, Bangkok 10330, Thailand*

[3]*Department of Physics, Faculty of Science, Kasetsart University, Bangkok 10900, Thailand*

(Received 8 October 2022; accepted 19 December 2022; published 27 January 2023)

The quadrupole normal-mode oscillation frequency f_n of a multiquark star are computed for $n = 1$–5. At the transition from low to high density multiquark in the core region, the first two modes jump to larger values, a distinctive signature of the presence of the high-density core. When the star oscillation couples with spacetime, gravitational waves (GW) will be generated and the star will undergo damped oscillation. The quasinormal modes (QNMs) of the oscillation are computed using two methods, direct scan and WKB, for QNMs with small and large imaginary parts respectively. The small imaginary QNMs have frequencies 1.5–2.6 kHz and damping times 0.19–1.7 secs for a multiquark star with mass $M = 0.6$–$2.1\ M_\odot$ (solar mass). The WKB QNMs with large imaginary parts have frequencies 5.98–9.81 kHz and damping times 0.13–0.46 ms for $M \simeq 0.3$–$2.1\ M_\odot$. They are found to be the fluid $f-$ modes and spacetime curvature $w-$ modes, respectively.

DOI: 10.1103/PhysRevD.107.023020

I. INTRODUCTION

The late-time gravitational waves signal from compact sources is prominently dominated by characteristic ringdown phase. This phase is described by a so-called quasinormal modes (QNMs). In principle, one can determine the nature of the source by measuring damping time of gravitational waves amplitude. Moreover, linear stabilities of compact objects can also be verified by the QNMs. An exponential decay of perturbation mode indicates that a perturbed object is stable under a linear perturbation. The studies of black hole quasinormal modes can be traced back to 1970, where Vishveshwara calculates an oscillation of a Gaussian wave packet around the Schwarzschild black hole [1]. It turns out that, the frequency and damping of these oscillations are solely characterized by its mass. Since then, numerous of a similar study have been explored with various types of black holes and fields (see Refs. [2–4] for a nice review on this subject). Beyond general relativity, QNMs of black holes in modified gravity are studied in great numbers. For instance, extended analyzes for black hole/string in massive gravity and generalized spherical symmetric background [5–9] demonstrate rich structure of the black hole QNMs and remarkable connections to the strong cosmic censorship.

Similarly, the study of stellar pulsation in general relativity has a long history [10–17]. In Refs. [18,19], a new family of oscillation modes of neutron stars are discovered, i.e., $w-$ modes or spacetime modes. The $w-$ modes are much closer to black hole QNMs than the fluid modes, i.e., f, p, g, and $r-$ modes. In addition, the $w-$ modes are oscillating with very rapid damping time. We refer an interested reader to Ref. [3] for a classification of neutron stars oscillation modes including subfamily of the spacetime modes. Moreover, the investigation of gravitational waves signal emitted from neutron stars can prove to be useful. It is expected that gravitational radiations from neutron stars carry information about the star's internal structure such as its radius, density, and properties of nuclear and quark matter [20–22].

There have been a series of investigations on the physical properties of massive neutron star (NS) with exotic quark-matter core in the form of multiquark (MQ) phase from the holographic Sakai-Sugimoto (SS) model [23–27]. There are also other types of holographic models, e.g., top-down models D3-D7, D4/D8/$\overline{\text{D8}}$ and a bottom-up V-QCD model considered in the study of neutron stars and hybrid stars [28–32]. In the top-down SS model, the dual gauge theory has many similar properties to the QCD, e.g., confinement/deconfinement phase transition, chiral symmetry breaking/restoration. Baryon can be added to the model by introduction of baryon vertex attached to N_c strings from the AdS boundary. Multiquark states can be constructed by adding equal numbers of string in and out of

*supakchai.p@gmail.com
†piyabut@gmail.com
‡quazact@gmail.com

the baryon vertex [24]. It is interesting that when the bulk spacetime contains horizon and the chiral symmetry is broken by the connecting D8-$\overline{\text{D8}}$ configuration, the multiquark phase is found to be the most thermodynamically preferred nuclear phase in the SS model for moderate temperature (less than $\times 10^{12}$ K) and high density [24]. Such physical condition is expected to be found in the core of massive compact astrophysical object such as neutron star. Consequently, aged massive NS above 2 solar masses is likely to contain the multiquark core and nuclear crust according to the SS model.

At the beginning of neutron star/hybrid star formation, e.g., after supernovae explosion, white dwarfs merging, excess mass intake of a neutron star; the resulting ultradense compact object could have an extremely high temperature, comparable to deconfinement phase transition temperature. In such circumstances, the compact star resulting from the collapse could be entirely in the deconfined MQ phase (or even contain quark-gluon plasma (QGP) core if core temperature is sufficiently large), where the coupling between quarks is still sufficiently strong to form bound states even when the quarks are deconfined within the much larger deconfined region. It is thus interesting to investigate the physical properties of massive compact stars entirely consisting of the MQ matter by assuming temperature at the star surface to be higher than the transition temperature between multiquark and ordinary nuclear matter. In Ref. [26], radial pulsations of the holographic MQ star have been analyzed and six characteristic frequency modes are determined.

In this work, we calculate the normal and quasinormal modes (QNMs) of holographic MQ stars in the SS model, in both the fluid-oscillation (Newtonian $f-$modes) and spacetime ($w-$modes) modes. By comparison to observations, these modes can be used to identify the MQ star/core with holographic equations of state in addition to other specific physical properties studied in Refs. [25–27]. The results can also be compared with frequencies of other possibilities of massive compact object such as strangeon stars (SS) [33] or other phases with different equations of state such as color-superconductivity (CSC) [34,35] (see Ref. [36] and references therein).

The work is organized as the following. Section II presents the equations of state (EoS) for holographic multiquark matter in the SS model and the perturbation equations of motion. Section III considers normal modes of fluid MQ star oscillation. QNMs for fluid and spacetime modes are calculated in Sec. IV. Section V concludes our work.

II. THEORETICAL SETUP: EQUATIONS OF STATE AND EQUATION OF MOTION

A. Equations of state

"Neutron stars" generically cool down rather quickly to temperatures lower than 0.1 MeV ($\sim 10^9$ K). At such moderate temperatures below the quark-gluon plasma formation, the coupling of strong interaction could still be strong. With extreme densities inside the neutron star, hadronic matters, e.g., neutrons and protons could not withstand extreme pressure, and the boundary between hadrons could overlap. Quarks inside one hadron might leak into others and could form multiquark bound states within an even larger confinement radius inside the star. During the earlier stage of the cool down process, the entire ultradense star could have temperature in the range $10^9\ \text{K} < T < 10^{12}$ K, where the holographic MQ phase is the most thermodynamically preferred phase (see Refs. [24,25]). During this period, the young "neutron star" could actually be the MQ star. And in the later time, the aged "NS" could actually be the hybrid star with MQ core. Another scenario where MQ star could be formed is when the massive NS gains more mass, collapses and heats up until most of the star is in the MQ phase.

At present, there is still no effective theory derived from QCD that could describe the hydrodynamic and thermodynamic behavior of the MQ states due to their strongly coupled nature. We thus adopt the EoS of MQ matter from holographic SS model originally computed in Ref. [23]. At high densities, the holographic MQ phase was found to be more thermodynamically preferred over the stiff nuclear matter described by chiral effective theory or CET in Ref. [25] and the KSZ(Kim-Sin-Zahed) models [37,38] in Ref. [27]. It should be noted that the MQ phase can be extended to include CSC when diquark condensate is formed at relatively low temperature, and include strange quark flavor to address the possibility of strange matter emergence, with and without the presence of strong coupling effects.

Correspondingly, the multiquark matter inside the star can be described by relations between pressure P and mass density ρ, written as a function of the number density n, as described in Ref. [23]. The EoS for the small n ("mql") multiquark can be expressed in the dimensionless form as

$$P = an^2 + bn^4,$$
$$\rho = \mu_0 n + an^2 + \frac{b}{3}n^4, \tag{1}$$

where μ_0 is the initial value of the chemical potential for the multiquark phase, while a, b are the parameters associated with the small n holographic multiquark EoS. On the other hand, for large n ("mqh")

$$P = kn^{7/5},$$
$$\rho = \rho_c + \frac{5}{2}P + \mu_c(n - n_c) + kn_c^{7/5} - \frac{7k}{2}n_c^{2/5}n, \tag{2}$$

where a critical mass density, chemical potential, and number density at the transition from large to small multiquark number density, represented by ρ_c, μ_c, and n_c, respectively.

TABLE I. Parameters associated with EoS expressed in Eqs. (1) and (2) in dimensionless units.

n_s	a	b	μ_0	k	ρ_c	μ_c	n_c
0	1	0	0.17495	$10^{-0.4}$	0.0841077	0.564374	0.215443
0.3	0.375	180.0	0.32767	$10^{-0.4}$	0.0345996	0.490069	0.086666

Equations (1) and (2) are expressed in dimensionless form where all parameters are provided in Table I. For both $n_s = 0$ and 0.3 cases, the parameter $k = 10^{-0.4}$. This implies that the MQ at high density is independent of the color charges as they have similar characteristics. Notably, these EoS are shown to be insensitive to temperature in the range $10^9\ \mathrm{K} < T < 10^{12}\ \mathrm{K}$ [23]. The EoS for multiquark depends on two free parameters: the color charge of the multiquark state n_s and the energy density scale ϵ_s [23,24]. Converting to SI units, the pressure P and mass density ρ are proportional to the energy density scale ϵ_s. As a result, the pure MQ-star mass and radius have the same scaling $M, R \sim \epsilon_s^{-1/2}$. Remarkably, the compactness M/R is thus unaffected by ϵ_s. In this work, we will set $\epsilon_s = 26\ \mathrm{GeV\,fm^{-3}}$.

B. Equations of motion

We use the convention of Refs. [18,19]. The metric is expressed as

$$\begin{aligned} ds^2 = &-e^{\nu}(1 + r^{\ell} H_0 Y_m^{\ell} e^{i\omega t})dt^2 - 2i\omega r^{\ell+1} H_1 Y_m^{\ell} e^{i\omega t} dt dr \\ &+ e^{\lambda}(1 - r^{\ell} H_0 Y_m^{\ell} e^{i\omega t})dr^2 \\ &+ r^2(1 - r^{\ell} K Y_m^{\ell} e^{i\omega t})(d\theta^2 + \sin^2\theta d\phi^2), \end{aligned} \tag{3}$$

where $\nu, \lambda, H_0, H_1, K$ are functions of radial coordinate r and the spherical harmonics is denoted by Y_m^{ℓ}. The fluid 4-velocity sourcing the spacetime perturbation for even parity modes are given by [13] (with r^{ℓ} rescaling),

$$\begin{aligned} &u^0 = e^{-\nu/2}\left(1 - \frac{1}{2} r^{\ell} H_0 Y_m^{\ell} e^{i\omega t}\right), \quad u^r = r^{\ell-1} e^{-(\nu+\lambda)/2} \partial_t W Y_m^{\ell}, \\ &u^{\theta} = -r^{\ell-2} e^{-\nu/2} \partial_t V \partial_{\theta} Y_m^{\ell}, \quad u^{\phi} = 0, \end{aligned} \tag{4}$$

where $W = W(t, r)$ and $V = V(t, r)$. Generally, perturbed Einstein field equations yield five first order differential equations for H_0, H_1, K, W, V. However, they are not all linear independent. In fact, the Einstein equation implies the following [18]

$$\begin{aligned} (2M + Nr + \bar{Q})H_0 = &-[(N+1)\bar{Q} - \omega^2 r^3 e^{-(\lambda+\nu)}]H_1 \\ &+ \left[Nr - \omega^2 r^3 e^{-\nu} - \frac{e^{\lambda}}{r}\bar{Q}(2M \right. \\ &\left. - r + \bar{Q})\right] K + 8\pi r^3 e^{-\frac{\nu}{2}} X, \end{aligned} \tag{5}$$

with $\bar{Q} = M + 4\pi r^3 P$ and $N = (\ell - 1)(\ell + 2)/2$. The new function X is introduced [16]

$$\begin{aligned} X \equiv &\omega^2 (P + \rho) e^{-\nu/2} V + \frac{(P + \rho)}{2} e^{\nu/2} H_0 \\ &- \frac{P'}{r} e^{(\nu-\lambda)/2} W. \end{aligned} \tag{6}$$

The equations of motion governing the perturbations of fluid in a spherically symmetric star with no rotation are given by the Einstein field equations,

$$\begin{aligned} H_1' = &\frac{e^{\lambda}}{r}\left(-[(\ell+1)e^{-\lambda} + 2\frac{M}{r} + 4\pi r^2 (P - \rho)]H_1 + H_0 + K \right. \\ &\left. - 16\pi (P + \rho) V\right), \\ K' = &\frac{1}{r}\left(H_0 + (N+1)H_1 - \left(\ell + 1 - \frac{r\nu'}{2}\right)K \right. \\ &\left. - 8\pi (P + \rho) e^{\lambda/2} W\right), \\ W' = &-(\ell+1) W r^{-1} + r e^{\lambda/2}\left(\frac{1}{2} H_0 + K + (\gamma P)^{-1} e^{-\nu/2} X \right. \\ &\left. - \ell(\ell+1) r^{-2} V\right), \\ X' = &-\frac{\ell}{r} X + \frac{1}{2r}(\rho + P) e^{\frac{\nu}{2}}\left[\left(1 - \frac{\nu' r}{2}\right) H_0 + (r^2 \omega^2 e^{-\nu} \right. \\ &+ (N+1)) H_1 + \left(\frac{3}{2}\nu' r - 1\right) K - \frac{\ell(\ell+1)\nu'}{r} V \\ &\left. - \left(8\pi(\rho + P) e^{\frac{\lambda}{2}} + 2\omega^2 e^{\frac{\lambda}{2} - \nu} - r^2 \left(\frac{\nu'}{r^2 e^{\frac{\lambda}{2}}}\right)'\right) W\right]. \end{aligned} \tag{7}$$

Remark that, we can eliminate H_0 and V using (5) and (6) respectively from the perturbation equations (7). Thus we obtain four first order differential equations for $\{H_1, K, W, X\}$.

We will solve these perturbation equations with appropriated boundary conditions. As a result, one obtains specific frequency ω. For the calculation of normal modes, the boundary condition at the star surface $r = R$ is simply $X(R) = 0$ (zero pressure and density at the surface) and there is no need to do the matching with the outer region of the star. The normal modes correspond to real frequency. Boundary conditions and numerical procedure for obtaining QNMs and their corresponding quasinormal frequency can be found below in Sec. IV.

III. NORMAL MODES OF MULTIQUARK STAR

In this section, the normal modes quadrupole oscillations and QNMs of the multiquark star are numerically calculated. The normal mode quadrupole oscillations are computed under the assumption that the energy loss to the gravitational waves is negligible and the frequency $f = \omega/2\pi$ is purely real. These Newtonian modes are simply fluid nonradial oscillations confined by gravity of the star with boundary conditions $X = 0$, $r \geq R$. In Figs. 1 and 2, the five lowest frequency modes ($n = 1$–5) are displayed as a function of MQ star's mass and star's compactness $C \equiv M/R$ respectively (note that the MQ star with mass smaller than 1.4 $M_\odot$ is most likely hypothetical but we choose to present them for comparison to the typical NS with other nuclear EoS). The frequencies are found to be monotonically increasing with M and C. At high mass $M \gtrsim 2\ M_\odot$ and compactness when the star has the high density "mqh" core, the behavior of the frequencies become nontrivial. The high-density core acquires its own fundamental oscillation resulting in the appearance of the lowest mode f_1. At the same time, the second mode jumps to higher value while f_4 and f_5 start to decrease with increasing M, C at higher masses while f_3 coincidentally stays monotonic. In the presence of very small Newtonian damping, these normal modes obtain very small imaginary part in the frequency and become the $f-$modes discussed in Sec. IV.

In comparison, typical $f-$mode frequencies of the neutron star with nuclear matter content are in the range 1.5–3 kHz [3,16] while the p_1-mode frequencies are around 4–7 kHz. For the multiquark star with masses around 1.4 solar masses, the f_2 is the lowest mode and its value is 2.6–2.7 kHz. The multiquark oscillation has relatively high fundamental frequency comparable to the nuclear matter with high mean density. This is consistent with the fact that the multiquark phase consists of extremely dense bound states of quarks. The "mql" multiquark behaves very similar to baryon. Only when the density becomes even higher that "mqh" multiquark EoS emerges and the most fundamental frequency f_1 appears in the massive multiquark star above 2 solar masses.

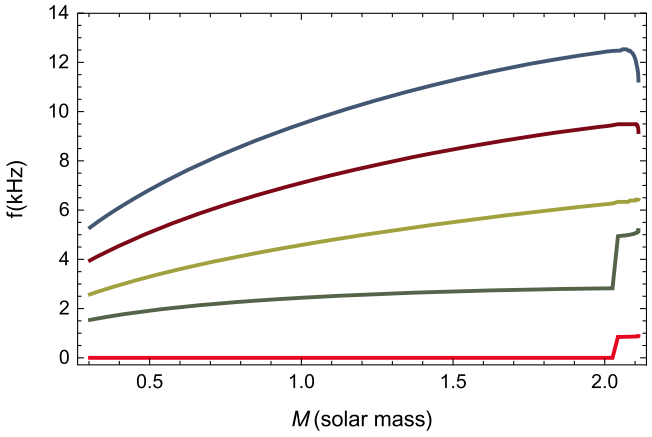

FIG. 1. Quadrupole oscillation frequency $f_n, n = 1, 2, 3, 4, 5$ vs M of the MQ star.

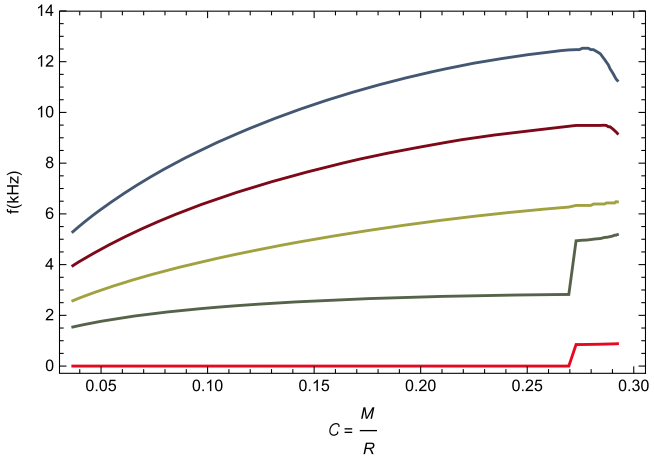

FIG. 2. Quadrupole oscillation frequency $f_n, n = 1, 2, 3, 4, 5$ vs compactness C of the MQ star.

IV. QUASINORMAL MODES OF MULTIQUARK STAR

For compact objects with extreme density, quadrupole oscillations of star can couple to the spacetime generating GWs which carry energy away. In this case, the oscillation will be damped resulting in the QNMs of the dense massive star. Depending on the physical modes, coupling between spacetime and fluid content of the star could be drastically different. While normal-mode quadrupole oscillations are $f-$modes, oscillatory modes with small spacetime-fluid coupling could have small imaginary parts of ω.

The QNMs are calculated using two methods, the direct scan and WKB. Both methods find solution with zero incoming waves. Direct scan is used to find the QNMs with very small $\mathrm{Im}\,\omega$, the ratio of incoming to outgoing waves are in the order of 10^{-6} at far distance $r = 55\,\mathrm{Re}\,\omega$. For WKB, the outer wave solutions of QNMs are verified that they contain less than 10^{-3} of the incoming/outgoing waves ratio at far distance $r > 50\,\mathrm{Re}\omega$. Figures 3–5 show real and imaginary parts of ω in dimensionless unit (note that the MQ star with mass smaller than 1.4 $M_\odot$ is most likely hypothetical but we choose to present them for comparison to the typical NS with other nuclear EoS). The value of $\mathrm{Re}\omega$ can be translated to the frequency f in the SI units by the conversion factor $f_{\mathrm{con}} \equiv 1.73603\sqrt{\epsilon_s/(\mathrm{GeV\,fm^{-3}})} = 8.85206$ kHz for $\epsilon_s = 26\ \mathrm{GeV/fm^3}$. The damping time $\tau \equiv 1/\mathrm{Im}\,\omega$ can be translated to time unit by the conversion factor $t_{\mathrm{con}} \equiv 0.01797943211$ ms (scales with $1/\sqrt{\epsilon_s}$).

A. The inner solution of the star

To ensure the condition $X(R) = 0$ is satisfied, we use the same procedure as Ref. [16] to solve Eqs. (7) in the form

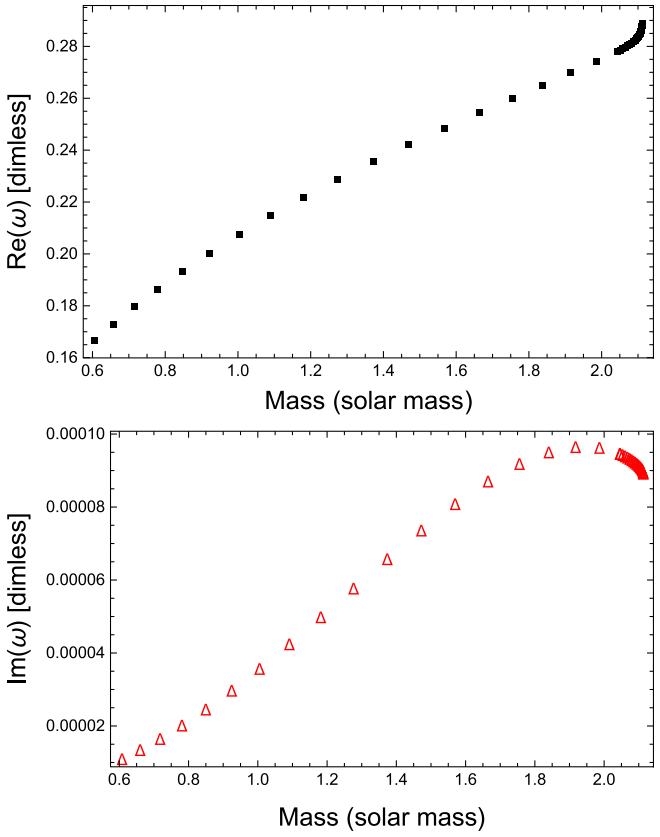

FIG. 3. QNMs with small Im ω vs mass of the MQ star.

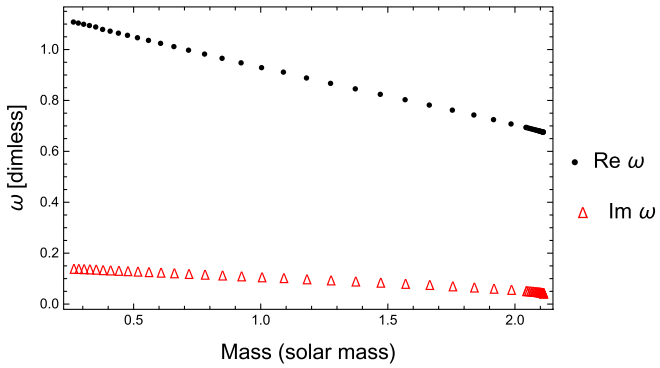

FIG. 4. QNMs vs mass of the MQ star.

$$\frac{d\mathbf{Y}}{dr} = \mathbf{P}(r, \ell, \omega) \cdot \mathbf{Y}, \tag{8}$$

where $\mathbf{Y} = (H_1, K, W, X)$ and the matrix $\mathbf{P}$ can be read off from (7) after using constraints from the equations of motion to eliminate V, H_0. Then three independent solutions with $X(R) = 0$ are numerically solved from the surface to the radius $r = R/2$ and two independent solutions are solved from the center out to $r = R/2$. The general solutions can be expressed as

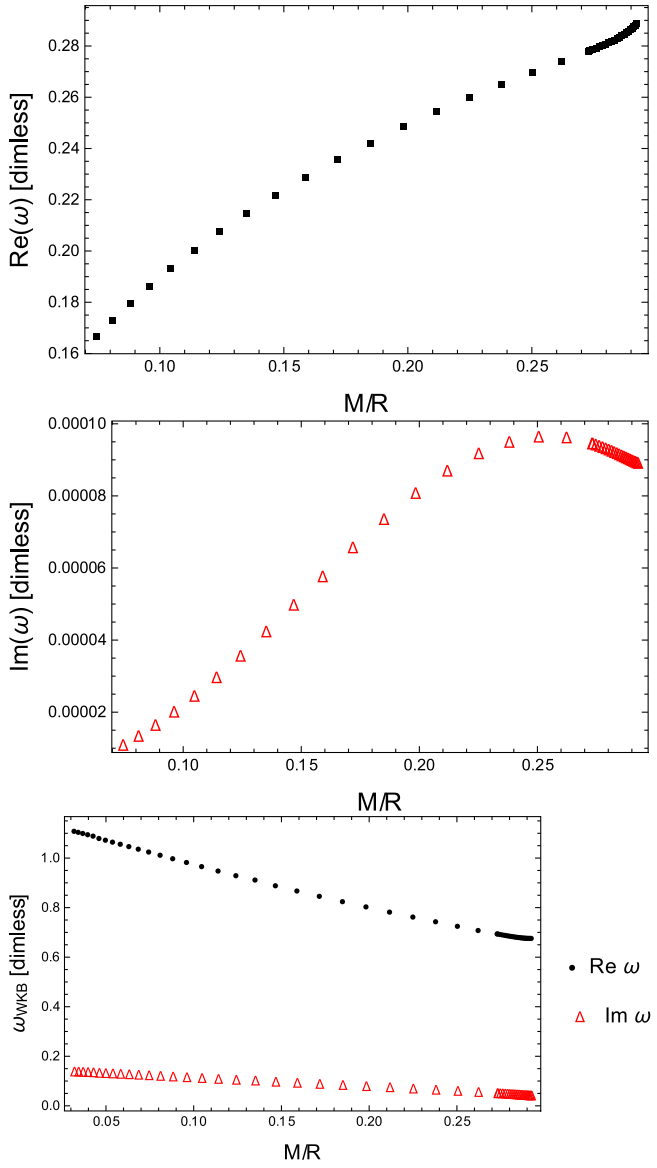

FIG. 5. QNMs with small Im ω and large (WKB) Im ω vs compactness M/R of the MQ star.

$$\mathbf{Y}_{\text{in}}(R/2 \le r \le R) = a_1\mathbf{Y}_1(r) + a_2\mathbf{Y}_2(r) + a_3\mathbf{Y}_3(r),$$
$$\mathbf{Y}_{\text{in}}(0 \le r \le R/2) = a_4\mathbf{Y}_4(r) + a_5\mathbf{Y}_5(r). \tag{9}$$

The physical inner solution requires the matching

$$a_1\mathbf{Y}_1(R/2) + a_2\mathbf{Y}_2(R/2) + a_3\mathbf{Y}_3(R/2) = a_4\mathbf{Y}_4(R/2) + a_5\mathbf{Y}_5(R/2). \tag{10}$$

B. The outer solutions

At surface of the star, the inner and outer solutions are matched via the transformation related to Zerilli function $Z(r_*)$

$$\begin{pmatrix} 0 & 1 \\ 1 & 0 \end{pmatrix} \begin{pmatrix} r^{-(\ell+1)} H_1(r) \\ r^{-\ell} K(r) \end{pmatrix} = \begin{pmatrix} f(r) & g(r) \\ h(r) & k(r) \end{pmatrix} \begin{pmatrix} Z(r_*) \\ Z'(r_*) \end{pmatrix}, \tag{11}$$

where $Z'(r_*) \equiv \frac{dZ}{dr_*}$,

$$f(r) = \frac{N(N+1)r^2 + 3NMr + 6M^2}{r^2(Nr+3M)}, \qquad g(r) = 1,$$
$$h(r) = \frac{-Nr^2 + 3NMr + 3M^2}{(r-2M)(Nr+3M)}, \qquad k(r) = \frac{-r^2}{r-2M},$$

and the tortoise coordinate r_* is

$$r_* = r + 2M \log\left(\frac{r}{2M} - 1\right). \tag{12}$$

Outside the star, there is no source of matter and the spacetime resembles the Schwarzschild metric. Therefore the perturbation equations reduce to a single wavelike equation [39]. Generically, the wave equation (Zerilli's equation) in the exterior of the star is given by

$$\frac{d^2Z}{dr_*^2} + (\omega^2 - V(r))Z = 0, \tag{13}$$

where the effective potential is

$$V(r) = \frac{2(1-2M/r)}{r^2(Nr+3M)^2} \times ((N+1)N^2r^3 + 3N^2Mr^2 + 9NM^2r + 9M^3). \tag{14}$$

For real ω, there are two linearly independent solutions to the Zerilli's equation,

$$Z_-(r_*) = e^{-i\omega r_*} \sum_{j=0}^{\infty} \alpha_j r^{-j},$$
$$Z_+(r_*) = e^{i\omega r_*} \sum_{j=0}^{\infty} \bar{\alpha}_j r^{-j}, \tag{15}$$

where $Z_-(Z_+)$ represents the purely outgoing (incoming) waves respectively. The coefficient $\bar{\alpha}_j$ is the complex conjugate of α_j, they can be found by the recursive relation (e.g., in Ref. [40]) using conventional Frobenius method. The generic solution in the outer region is then given by

$$Z_{\text{out}} = A(\omega)Z_- + B(\omega)Z_+, \tag{16}$$

where the ratio $B(\omega)/A(\omega) = 1$, 0 for normal and quasinormal modes respectively.

C. QNMs with small Im ω

A method although laborious yet effective in finding the QNMs with small imaginary parts is to scan for solution with $B(\omega)/A(\omega) = 0$ by varying ω.

The results are shown in Fig. 3. These modes have less than 10^{-6} of the incoming/outgoing waves ratio at far distance $r = 55\,\mathrm{Re}\,\omega$. As the MQ-star mass increases, the real and imaginary part of quasinormal frequencies increase with the MQ-star mass. Interestingly, polar QNMs of neutron star in massive scalar-tensor gravity also share a similar trend [41].

D. WKB

For the WKB method, the approximate wave solution is given by replacement $Z_\mp \to Z_\mp^{\text{WKB}}$ where

$$Z_\mp^{\text{WKB}}(r) = Q(r_*)^{1/2} \exp\left[\mp i \int^{r_*} Q(y)dy\right], \tag{17}$$

and

$$Q(r_*) = (\omega^2 - V(r))^{1/2}$$

in Eq. (16) respectively. The ratio of the incoming and outgoing waves is thus [18]

$$\frac{B(\omega)}{A(\omega)} = e^{-2iQ(R)} \frac{Q(R) - i\left[\frac{Z'_{\text{in}}(R)}{Z_{\text{in}}(R)} + \frac{Q'(R)}{2Q(R)}\right]}{Q(R) + i\left[\frac{Z'_{\text{in}}(R)}{Z_{\text{in}}(R)} + \frac{Q'(R)}{2Q(R)}\right]}, \tag{18}$$

where the prime indicates derivative with respect to r_*. The QNMs can be determined by numerical evaluation of the roots of $B(\omega)/A(\omega) = 0$, by first substituting a trial value of ω and solve for the inner solution $Z_{\text{in}}(r)$ within the star. The resulting roots for ω is then fed back to the equation of motion to find a new inner solution and repeat the process until ω converges to a single value. Figure 4 shows QNMs of multiquark star with large Imω determined by the WKB method, the physical value scales with $\sqrt{\epsilon_s}$. In contrast to Fig. 3, the real and imaginary part of quasinormal frequencies decrease monotonically with the MQ-star mass. Similar behavior is found for the axial perturbation of neutron star in R^2 gravity [42].

In order to understand more on the physical origin of the two kinds of modes, we plot ω versus compactness M/R in Fig. 5. The small-Im ω modes have Re ω increasing with compactness while Im ω increases with C until a maximum around $C \simeq 0.25$–0.26 then it decreases. In contrast, WKB modes (with large Im ω) have ω as a decreasing function of C for both real and imaginary parts. Re ω and Im ω can be converted to SI units by conversion factors f_{con} and t_{con}, respectively.

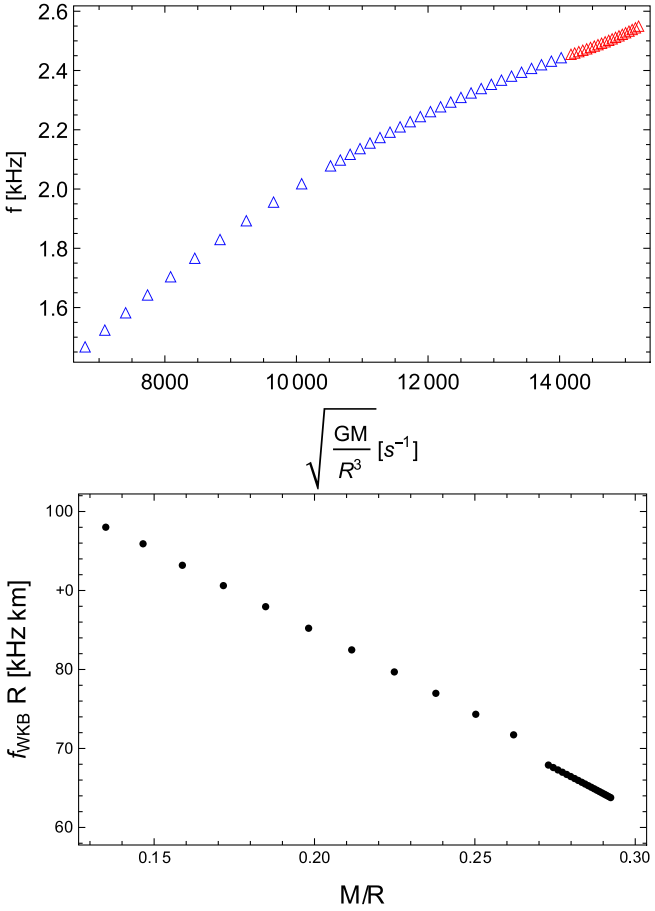

FIG. 6. Frequencies $f = \mathrm{Re}\,\omega/2\pi$ of $f-$modes vs $\sqrt{G\bar{\rho}}$ (upper) and fR of WKB $w-$modes vs C (lower). The red/dense dots on the high C values show MQ star with high-density "mqh" core.

In addition, the small imaginary modes (the upper two plots in Fig. 5) appear to follow the universal relations of QNMs of neutron star reported in [20] in a small compactness region, i.e., $C < 0.25$. However, our results on the WKB modes do not share the universality found in [20].

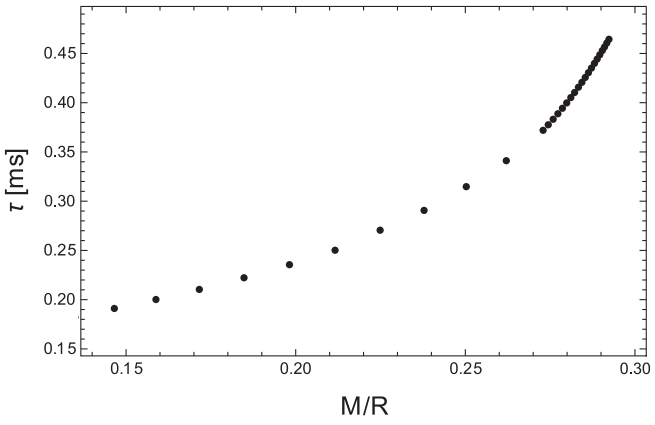

FIG. 7. Damping time τ of WKB $w-$modes vs C. The dense dots on the high C values show MQ star with high-density "mqh" core.

This discrepancy may allow us to distinguish the gravitational radiation from the MQ star.

From the range of numerical values of the QNMs for both kinds and the approximate linear behavior of the frequencies shown in Fig. 6 ($\bar{\rho} = M/R^3$, average density of the star), we can conclude that the small-Imω modes are the $f-$modes, and the WKB QNMs are the curvature $w-$modes according to the criteria in Refs. [3,43]. Moreover, the damping time of the WKB modes is an increasing function of compactness as shown in Fig. 7, consistent with the property of the curvature $w-$modes. The spacetime metric perturbations H_1, K of these modes clearly are dominant as shown in Appendix A.

V. CONCLUSIONS AND DISCUSSIONS

The oscillatory modes of holographic MQ star/core of massive stars in the SS model with the energy density scale $\epsilon_s = 26$ GeV fm^{-3} have been calculated. We obtain normal and quasinormal modes of MQ star by using direct scan and WKB methods. We find that the stars with higher mass and compactness oscillate with higher frequencies. By direct scanning of the solutions satisfying boundary condition of the quasinormal modes, i.e., zero incoming gravitational waves from infinity in the outer region of star, QNMs with very small Im ω are found with frequencies in the order of 1.5–2.6 kHz, and damping times 0.19–1.7 s for MQ star with mass $M = (0.6-2.1)\ M_\odot$ (note that the MQ star with mass smaller than 1.4 $M_\odot$ is most likely hypothetical, however we choose to present them for comparison to the typical NS with other nuclear EoS). By using WKB method, QNMs with larger Im ω are found with $f = 5.98$–9.81 kHz, damping times 0.13–0.46 ms for $M \simeq (0.3-2.1)\ M_\odot$. These are the $f-$modes and curvature $w-$modes of MQ star respectively. Both modes can be fit with approximate empirical linear relations found in Ref. [43] as shown in Fig. 6. For MQ $f-$modes, since the EoS is not a single power law, the approximate linear relation can fit well only around the high mass region of the star in Fig. 6. For $w-$modes, the linear relation fit is quite excellent even though there appears to be a transition from one fitting linear relation to another when the MQ star changes from the star with high density "mqh" core to pure "mql" star.

Massive neutron star around and above two solar masses could have multiquark core whence further gravitational collapse would generate fluid and spacetime excitations in the f, p, g, r, and $w-$modes. The GW from these excitations could be detected after such collapse, e.g., in aftermath of supernovae explosion and neutron stars collision. It is thus possible that these QNMs would be generated by such extreme events and subsequently detected at LIGO/Virgo and future gravitational waves detection facilities. The sensitivities of these GW events are estimated in Appendix B.

ACKNOWLEDGMENTS

S. P. (first author) was supported by Grant No. RGNS 64-217 from Office of the Permanent Secretary, Ministry of Higher Education, Science, Research and Innovation (OPS MHESI), Thailand Science Research and Innovation (TSRI) and Silpakorn University. P. B. is grateful to APCTP for warm hospitality during the visit where part of this work has been done.

APPENDIX A: PERTURBATION PROFILES OF WKB $H_1(r)$, $K(r)$, $W(r)$, $X(r)$ INSIDE THE MQ STAR

Perturbations inside the MQ star for the WKB modes (spacetime curvature $w-$modes) at $M = 2.04\ M_\odot$ (where "mqh" disappears and only "mql" exists) MQ star are shown in Fig. 8. The spacetime metric perturbations H_1, K are clearly dominant for this mode.

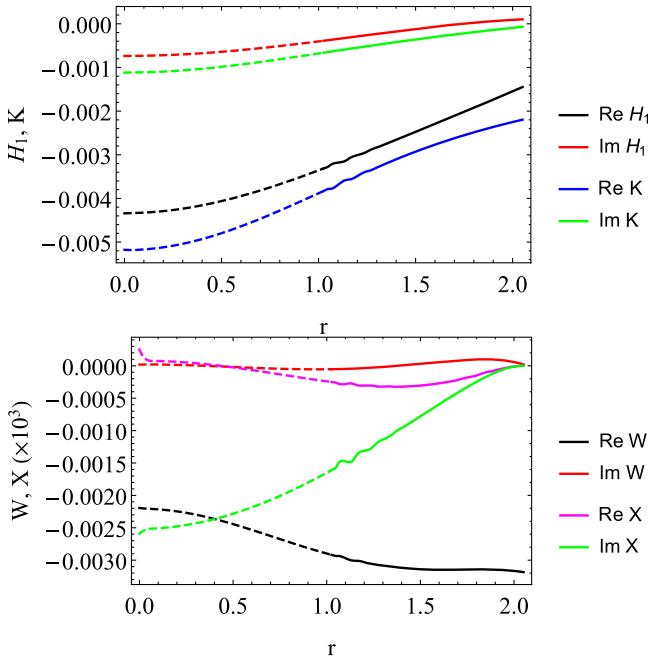

FIG. 8. Perturbations inside MQ star for WKB mode at $M = 2.04\ M_\odot$, note that the value of X is multiplied by 10^3.

APPENDIX B: SENSITIVITY OF GW SIGNALS FROM $f-$MODE AND $w-$MODE OSCILLATIONS OF MQ STAR

In order to estimate the sensitivities of GW from oscillating MQ star at the detection facilities, we adapt the approximation formula for GW amplitude $h_{\rm eff}$ by Andersson and Kokkotas [43,44],

$$h_{\rm eff} \sim 2.2\times 10^{-21}\left(\frac{E}{10^{-6}\ M_\odot c^2}\right)^{1/2}\left(\frac{2\ \text{kHz}}{f}\right)^{1/2}\left(\frac{50\ \text{kpc}}{r}\right), \tag{B1}$$

and

$$h_{\rm eff} \sim 9.7\times 10^{-22}\left(\frac{E}{10^{-6}\ M_\odot c^2}\right)^{1/2}\left(\frac{10\ \text{kHz}}{f}\right)^{1/2}\left(\frac{50\ \text{kpc}}{r}\right) \tag{B2}$$

for the $f-$mode and $w-$mode respectively. E is the available energy in GW form and r is the distance to the source.

The sensitivity at a detector is then given by $\text{strain}/\sqrt{\text{Hz}} \simeq h_{\rm eff}/10\sqrt{\text{Hz}}$ for signal bandwidth 100 Hz. For $M = M_{\rm max} = 2.11\ M_\odot$, the lowest $f-$mode ($w-$mode) $f = 2.55(5.98)$ kHz, the required minimum sensitivity for detection is $1.54(1.0)\times 10^{-24}/\sqrt{\text{Hz}}$ for $E = 10\times 10^{-6}\ M_\odot c^2$, $r = 20$ Mpc respectively. Large uncertainties come from the amount of available energy in each mode of GW since $h_{\rm eff} \sim \sqrt{E}$. With our estimate of $E = 10\times 10^{-6}\ M_\odot c^2$ and by comparison to Table II, the GW signals in these modes are still beyond the discovery sensitivity of present detection facilities, LIGO/Virgo, for nearby source at 20 Mpc (half the distance of GW170817). However, the future detection facilities such as the Einstein Telescope and Cosmic Explorer have the potential to discover GW signals from these modes for events with $E \sim 10\times 10^{-6}\ M_\odot c^2$ at 20 Mpc.

TABLE II. Minimum sensitivity at the lowest $f-$mode and $w-$mode MQ star frequencies at present and future detection facilities estimated from Fig. 1 of Ref. [45].

Minimum sensitivity $(1/\sqrt{\text{Hz}})$ (at)	Advanced LIGO/Virgo	Einstein Telescope	Cosmic Explorer
2.55 kHz	$\gtrsim 1\times 10^{-23}$	$\gtrsim 1\times 10^{-24}$	1×10^{-24}
5.98 kHz	$\gtrsim 3\times 10^{-23}$	$\gtrsim 3\times 10^{-24}$	2×10^{-24}

[1] C. V. Vishveshwara, Nature (London) **227**, 936 (1970).
[2] R. A. Konoplya and A. Zhidenko, Rev. Mod. Phys. **83**, 793 (2011).
[3] K. D. Kokkotas and B. G. Schmidt, Living Rev. Relativity **2**, 2 (1999).
[4] V. Ferrari and L. Gualtieri, Gen. Relativ. Gravit. **40**, 945 (2008).
[5] P. Burikham, S. Ponglertsakul, and L. Tannukij, Phys. Rev. D **96**, 124001 (2017).
[6] S. Ponglertsakul, P. Burikham, and L. Tannukij, Eur. Phys. J. C **78**, 584 (2018).

[7] S. Ponglertsakul, P. Burikham, and T. Tangphati, Phys. Rev. D **99**, 084002 (2019).
[8] T. Wuthicharn, S. Ponglertsakul, and P. Burikham, Int. J. Mod. Phys. D **31**, 2150127 (2022).
[9] P. Burikham, S. Ponglertsakul, and T. Wuthicharn, Eur. Phys. J. C **80**, 954 (2020).
[10] G. Chanmugam, Astrophys. J. **217**, 799 (1977).
[11] J. R. Ipser and R. Semenzato, Astrophys. J. **229**, 1098 (1979).
[12] K. S. Thorne, Phys. Rev. Lett. **21**, 320 (1968).
[13] K. S. Thorne and A. Campolattaro, Astrophys. J. **149**, 591 (1967).
[14] R. Price and K. S. Thorne, Astrophys. J. **155**, 163 (1969).
[15] K. S. Thorne, Astrophys. J. **158**, 1 (1969).
[16] L. Lindblom and S. L. Detweiler, Astrophys. J. Suppl. Ser. **53**, 73 (1983).
[17] Y. Kojima, S. Yoshida, and T. Futamase, Prog. Theor. Phys. **86**, 401 (1991).
[18] K. D. Kokkotas and B. F. Schutz, Mon. Not. R. Astron. Soc. **255**, 119 (1992).
[19] N. Andersson, K. D. Kokkotas, and B. F. Schutz, Mon. Not. R. Astron. Soc. **274**, 1039 (1995).
[20] L. K. Tsui and P. T. Leung, Mon. Not. R. Astron. Soc. **357**, 1029 (2005).
[21] O. Benhar, E. Berti, and V. Ferrari, Mon. Not. R. Astron. Soc. **310**, 797 (1999).
[22] K. D. Kokkotas, T. A. Apostolatos, and N. Andersson, Mon. Not. R. Astron. Soc. **320**, 307 (2001).
[23] P. Burikham, E. Hirunsirisawat, and S. Pinkanjanarod, J. High Energy Phys. 06 (**2010**) 040.
[24] P. Burikham, A. Chatrabhuti, and E. Hirunsirisawat, J. High Energy Phys. 05 (2009) 006.
[25] S. Pinkanjanarod and P. Burikham, Eur. Phys. J. C **81**, 705 (2021).
[26] S. Pinkanjanarod, P. Burikham, and S. Ponglertsakul, Eur. Phys. J. C **82**, 141 (2022).
[27] P. Burikham, S. Pinkanjanarod, and S. Ponglertsakul, Phys. Rev. D **105**, 104018 (2022).
[28] C. Hoyos, N. Jokela, and A. Vuorinen, Prog. Part. Nucl. Phys. **126**, 103972 (2022).
[29] M. Järvinen, Eur. Phys. J. C **82**, 282 (2022).
[30] C. Hoyos, D. Rodríguez Fernández, N. Jokela, and A. Vuorinen, Phys. Rev. Lett. **117**, 032501 (2016).
[31] N. Jokela, M. Järvinen, and J. Remes, Phys. Rev. D **105**, 086005 (2022).
[32] T. Alho, J. Remes, K. Tuominen, and A. Vuorinen, Phys. Rev. D **101**, 106025 (2020).
[33] H. B. Li, Y. Gao, L. Shao, R. X. Xu, and R. Xu, Mon. Not. R. Astron. Soc. **516**, 6172 (2022).
[34] K. Fukushima and H. J. Warringa, Phys. Rev. Lett. **100**, 032007 (2008).
[35] B. Feng, D. Hou, H. c. Ren, and P. p. Wu, Phys. Rev. Lett. **105**, 042001 (2010).
[36] M. G. Alford, A. Schmitt, K. Rajagopal, and T. Schäfer, Rev. Mod. Phys. **80**, 1455 (2008).
[37] K. Y. Kim, S. J. Sin, and I. Zahed, J. High Energy Phys. 01 (2008) 002.
[38] K. Y. Kim, S. J. Sin, and I. Zahed, J. High Energy Phys. 09 (2008) 001.
[39] F. J. Zerilli, Phys. Rev. Lett. **24**, 737 (1970).
[40] S. Chandrasekhar and S. L. Detweiler, Proc. R. Soc. A **344**, 441 (1975).
[41] J. L. Blázquez-Salcedo, F. S. Khoo, J. Kunz, and V. Preut, Front. Phys. **9**, 741427 (2021).
[42] J. L. Blázquez-Salcedo, D. D. Doneva, J. Kunz, K. V. Staykov, and S. S. Yazadjiev, Phys. Rev. D **98**, 104047 (2018).
[43] N. Andersson and K. D. Kokkotas, Mon. Not. R. Astron. Soc. **299**, 1059 (1998).
[44] N. Andersson and K. D. Kokkotas, Phys. Rev. Lett. **77**, 4134 (1996).
[45] D. Martynov, H. Miao, H. Yang, F. H. Vivanco, E. Thrane, R. Smith, P. Lasky, W. E. East, R. Adhikari, A. Bauswein *et al.*, Phys. Rev. D **99**, 102004 (2019).